

Probing ϕ N interaction through bound states of ${}^6_\phi\text{He}$ mesic nuclei within ϕ N- α cluster model

Faisal Etminan*

*Department of Physics, Faculty of Sciences,
University of Birjand, Birjand 97175-615, Iran and
Interdisciplinary Theoretical and Mathematical Sciences
Program (iTHEMS), RIKEN, Wako 351-0198, Japan*

(Dated: July 24, 2025)

The spin dependence of the ϕ N interaction is explored through the bound states of ϕ N- α mesic nuclei with α being a spectator to attract the ϕ N pair without changing its spin structure. The bound state of ${}^6_\phi\text{He}$ mesic nuclei is calculated within the framework of the developed three-body cluster model by solving the Faddeev equations in the method of hyperspherical harmonics (HH) expansions. The calculations are done by employing the state-of-the-art ϕ N potential obtained from lattice QCD calculations and correlation function analysis for the ${}^4S_{3/2}$ and ${}^2S_{1/2}$ channels. The $\phi\alpha$ potential is constructed through a folding procedure of the spin-averaged ϕ N interaction with the matter distribution of ${}^4\text{He}$. And for $\text{N}\alpha$ potential two common types of $\text{N}\alpha$ interactions are taken from the literature with central and spin-orbit components. The central binding energies of the ϕ N- α bound states in the spin $3/2(1/2)$ channel are found to be $\sim 10(25)$ and $11(13)$ MeV at Euclidean times $t/a = 12$ and 14 , respectively. As well as, the corresponding nuclear matter radii are estimated to be $\sim 4.5(1.7)$ and $4.6(1.8)$ fm.

I. INTRODUCTION

Among the various studies of meson properties in nuclear matter, particular attention has been given to the vector ϕ -meson, since the interactions of the $s\bar{s}$ pair with nucleons and nuclei are not yet fully understood at low energies. Recently, ϕ -mesic nuclei—exotic

* fetminan@birjand.ac.ir

many-body systems characterized by strong interactions—have garnered renewed interest. The coupling of the ϕ meson to nucleons suggests that the stable formation of ϕ -mesic nuclei is probable, and both theoretical models and experimental efforts continue to investigate this possibility [1–8].

It has been established that the properties of the ϕ meson can be affected by the nuclear medium, resulting in behavior that differs from that observed in free space. The aim of numerous past and upcoming experiments is to explore how the ϕ meson behaves at finite densities [9, 10]. The primary issues addressed include whether the ϕ meson is indeed bound within nuclei, the magnitude of the binding energy, and the properties of such bound states. Additional focus is given to the possible modifications of the ϕ meson within nuclear matter and their potential detection in experiments. Theoretically, the properties of the ϕ meson in nuclear matter have been analyzed based on hadronic models [11], QCD sum rules [12], and effective Lagrangian approaches [13].

One of the simplest candidates for ϕ -mesic nuclei is the ϕ - NN system [5, 6, 14–17]. Recently, Filikhin et al. [7] studied the ϕ -mesic nuclei ${}^9_{\phi}\text{Be}$ and ${}^6_{\phi\phi}\text{He}$ within a three-body cluster model framework, treating them as $\phi\alpha\alpha$ and $\phi\phi\alpha$ systems using the Faddeev formalism in configuration space. The $\phi\alpha$ potential was determined through a folding procedure of the HAL QCD ϕN interaction in the ${}^4S_{3/2}$ channel [18], utilizing the matter distribution of ${}^4\text{He}$ [19].

Thanks to advancements in the HAL QCD methods [20–23] and the progress of high-performance computing facilities, hadron-hadron interactions have been obtained from first-principles lattice QCD simulations at near-physical quark masses [24]. These include interactions such as $\Lambda\Lambda$, ΞN [22], ΩN [25], $\Omega\Omega$ [26], $\Omega_{ccc}\Omega_{ccc}$ [27], $N-c\bar{c}$ [28], and ϕN [18]. The ϕN potential in the ${}^4S_{3/2}$ channel (with the notation ${}^{2s+1}L_J$, s is total spin, L orbital angular momentum, and J is total angular momentum) has been derived using a $(2 + 1)$ -flavor approach with quark masses near the physical point, on a sufficiently large lattice of size $L^3 = (8.1 \text{ fm})^3$. The corresponding isospin-averaged masses for π , K , ϕ , and N are 146, 525, 1048, and 954 MeV, respectively.

On the experimental side, the correlation function of proton- ϕ in heavy-ion collisions has been measured by the ALICE collaboration [29], providing the first experimental evidence of the attractive strong interaction between a proton and a ϕ -meson. Furthermore, based on the findings in Refs. [18, 29], available lattice data for the spin $3/2$ ϕN interaction obtained

by the HAL QCD collaboration [18] have been used in Ref. [30] to constrain the spin 1/2 counterpart through the fitting of the experimentally measured $p\phi$ correlation function by ALICE [29].

Since the experimental investigations to date have provided limited insights into the spin decomposition of the ϕN interaction (the measurement of the $p\phi$ scattering parameters are currently limited to spin averaged quantities [30]) the theoretical exploration of possible methods to perform this decomposition becomes essential. Accordingly, the properties of ϕ - $N\alpha$ -mesic nuclei are examined using the modern ϕN potential in the ${}^4S_{3/2}$ and ${}^2S_{1/2}$ channels, with α acting as a spectator, by employing advanced few-body computational techniques.

In this study, the binding energies and matter radii of ϕ - $N\alpha$ -mesic nuclei are calculated within a cluster model utilizing the hyperspherical harmonics (HH) expansion method [31–33]. Two types of $N\alpha$ interactions are considered: the first being the Sack-Biedenharn-Breit (SBB) $V_{n\alpha}$ potential [34], characterized by a Gaussian form, and the second employing a Woods-Saxon (WS) form used in coordinate space Faddeev calculations [31, 35].

The organization of this paper is as follows. In Section II, a brief outline of the three-body hyperspherical basis formalism is provided. The choices of the ϕ - N and ϕ , N -core interactions are discussed in Section III. Additionally, the $\phi\alpha$ potential, based on a Woods-Saxon fit of the folding of the HAL QCD spin-averaged ϕN interaction, is presented. In Section IV, the numerical results of the calculations for ϕ - $N\alpha$ mesic nuclei in the ${}^4S_{3/2}$ and ${}^2S_{1/2}$ channels are detailed. The final section, Section V, is dedicated to a summary and concluding remarks.

II. EXPANSION ON HYPERSPHERICAL HARMONICS (HH)

The expansion on hyperspherical harmonics method is developed version of the Faddeev equations in coordinate space. Since this method has been explained in details in other works [31, 36, 37], I shall here give a rather brief description of this formalism.

In a three-body $\phi+N$ +core model, the total three-body wave function Ψ is sum of three components, i.e., the (usually) inactive core intrinsic wave function and the active part that it depends on the relative coordinates and spins (often suppressed) of the two valence particles, $\Psi^{(i)}$, i.e., $\Psi = \sum_{i=1}^3 \Psi^{(i)}$. The components $\Psi^{(i)}$ are function of the three different

sets of Jacobi coordinates, One of the three sets is shown in the Fig. 1, and they satisfy the three Faddeev coupled equations,

$$(T - E) \Psi^{(i)} + V_{jk} (\Psi^{(i)} + \Psi^{(j)} + \Psi^{(k)}) = 0, \quad (1)$$

where T is the kinetic energy, E is the total energy, $V_{jk}(r_{jk})$ is the two body interactions between the corresponding pair and the indexes i, j, k is a cyclic permutation of $(1, 2, 3)$.

It is convenient to introduce translation invariant sets of Jacobi coordinates, $\{\vec{x}, \vec{y}\}$ illustrated in Fig. 1, are employed to describe three-body systems [six-dimensional problems]. The variable \vec{x} represents the relative coordinates between two of the particles and \vec{y} is between their center of mass and the third particle, $\vec{x}_i = \sqrt{A_{jk}} \vec{r}_{jk}$ and $\vec{y}_i = \sqrt{A_{(jk)i}} \vec{r}_{(jk)i}$ where $\vec{r}_{jk} = \vec{r}_j - \vec{r}_k$, $\vec{r}_{(jk)i} = \vec{r}_i - (A_j \vec{r}_j + A_k \vec{r}_k) / (A_j + A_k)$ with the scaling mass factor are defined by

$$A_{jk} = \frac{A_j A_k}{A_j + A_k}, \quad A_{(jk)i} = \frac{(A_j + A_k) A_i}{A_i + A_j + A_k}, \quad (2)$$

where $A_i = m_i/m$ with $m = 1$ a.m.u. and m_i the mass of particle i in a.m.u. The Jacobi coordinates are transformed into the hyperspherical coordinates $\{\rho, \alpha, \Omega_x, \Omega_y\}$, with hyperradius $\rho^2 = x^2 + y^2$ and the hyperangle $\alpha = \arctan(x/y)$. The angles Ω_x and Ω_y , which define the directions of the vectors \vec{x} and \vec{y} respectively, are described. For simplicity, all angular dependencies are expressed through $\varphi = (\alpha, \Omega_x, \Omega_y)$. The Hamiltonian of a

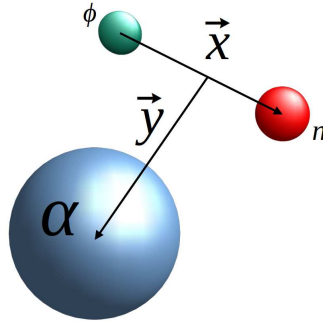


FIG. 1: The Jacobi T-coordinate system used to describe the ${}^6_\phi\text{He}$ mesic nuclei as $\phi\text{N}-\alpha$.

three-body system in hyperspherical coordinates is given by

$$\hat{H} = \hat{T}(\rho, \varphi) + \hat{V}(\rho, \varphi), \quad (3)$$

where the potential operator $\hat{V}(\rho, \varphi)$, representing the sum of pairwise interactions, is included, and the free Hamiltonian operator $\hat{T}(\rho, \varphi)$ is defined as in Ref. [38]

$$\hat{T}(\rho, \varphi) = -\frac{\hbar^2}{2m} \left(\frac{\partial^2}{\partial \rho^2} + \frac{5}{\rho} \frac{\partial}{\partial \rho} - \frac{1}{\rho^2} \hat{K}^2(\varphi) \right), \quad (4)$$

where the hyperangular momentum operator, \hat{K} , which is regarded as a generalized angular momentum operator, is introduced. The mass m , chosen as the normalization mass, is noted to be $m = m_N$.

Solutions to the Schrödinger equation with the three-body Hamiltonian given in Eq. (3) can be expanded for each ρ , with the total angular momentum j considered, as

$$\psi_{i\beta}^{j\mu}(\rho, \varphi) = R_{i\beta}(\rho) \mathcal{Y}_{\beta}^{j\mu}(\varphi), \quad (5)$$

where the functions $\mathcal{Y}_{\beta}^{j\mu}(\varphi)$ form a complete set of hyperangular functions. These functions are expanded in hyperspherical harmonics as presented in Refs. [31, 32, 36], and the hyperradial functions $R_{i\beta}(\rho)$ are introduced, with the subscript i indicating the hyperradial excitation. To facilitate the solution of the coupled equations (7), the hyperradial functions, denoted as $\mathcal{R}_{\beta}^j(\rho)$, are expanded in an orthonormal discrete basis up to i_{\max} [37].

The set of quantum numbers $\beta \equiv \{K, l_x, l_y, l, S_x, j_{ab}\}$ is used, where l_x and l_y are the orbital angular momenta associated with the Jacobi coordinates \vec{x} and \vec{y} respectively. The total orbital angular momentum l is given by the sum $l_x + l_y$, and the total spin of the particle pair linked via \vec{x} , S_x , is included. The quantum number $j_{ab} = l + S_x$ is used, and the total angular momentum j is expressed as $j = j_{ab} + I$, with I indicating the spin of the third particle.

The wave functions of the system are defined as

$$\begin{aligned} \Psi^{j\mu}(\rho, \varphi) &= \sum_{\beta} \sum_{i=0}^{i_{\max}} C_{i\beta}^j \psi_{i\beta}^{j\mu}(\rho, \varphi) \\ &= \sum_{\beta} \left(\sum_{i=0}^{i_{\max}} C_{i\beta}^j R_{i\beta}(\rho) \right) \mathcal{Y}_{\beta}^{j\mu}(\varphi) = \sum_{\beta} \mathcal{R}_{\beta}^j(\rho) \mathcal{Y}_{\beta}^{j\mu}(\varphi), \end{aligned} \quad (6)$$

where the coefficients $C_{i\beta}^j$ are obtained through diagonalization of the three-body Hamiltonian within the basis functions up to i_{\max} . The hyperradial wave functions $\mathcal{R}_{\beta}(\rho)$ are solutions to the coupled differential equations, expressed as

$$\left(-\frac{\hbar^2}{2m} \left(\frac{d^2}{d\rho^2} - \frac{(K+3/2)(K+5/2)}{\rho^2} \right) - E \right) \mathcal{R}_{\beta}^j(\rho) + \sum_{\beta'} V_{\beta'\beta}^{j\mu}(\rho) \mathcal{R}_{\beta'}^j(\rho) = 0, \quad (7)$$

where the term $V_{\beta'\beta}^{j\mu}(\rho)$, associated with two-body potentials between pairs of particles (V_{ij}), is defined by

$$V_{\beta'\beta}^{j\mu}(\rho) = \langle \mathcal{Y}_{\beta}^{j\mu}(\varphi) | V_{12} + V_{13} + V_{23} | \mathcal{Y}_{\beta'}^{j\mu}(\varphi) \rangle. \quad (8)$$

Calling r the modulus of the coordinate relating two particles, the general binary interaction potential, involving central, spin-orbit, spin-spin, and tensor components, is characterized by

$$\hat{V}_{ij} = V_c(r) + V_{so}(r) \vec{l}_{ij} \cdot \vec{s}_{ij} + V_{ss}(r) \vec{s}_i \cdot \vec{s}_j + V_T(r) \hat{S}_{ij}, \quad (9)$$

where \vec{s}_i denotes the spin of particle i , and $\vec{s}_{ij} \equiv \vec{s}_i + \vec{s}_j$. The relative orbital angular momentum between particles i and j is represented by \vec{l}_{ij} , while \hat{S}_{ij} stands for the tensor operator. The radial form factors for each term may be chosen from functions such as Gaussian, exponential, Woods-Saxon, or Yukawa functions.

III. CHOICE OF ϕ N AND N-CORE INTERACTIONS

The unique aspect of the three-body problem lies in its sensitivity to the off-shell behavior of the two-body interaction. To examine this, various choices of ϕ N and N α interactions were employed in calculations of ϕ N- α systems.

A. ϕ N potentials

As reported in Ref. [18], the ϕ N ($^4S_{3/2}$) potential is characterized by a combination of an attractive core at short distances and a two-pion-exchange (TPE) tail at long distances, with an overall strength proportional to m_π^4 . Utilizing the HAL QCD method, it was found that the ϕ N correlation function is predominantly influenced by elastic scattering states in the $^4S_{3/2}$ channel, with no significant contributions from the two-body channels ΛK ($^2D_{3/2}$) and ΣK ($^2D_{3/2}$), nor from three-body open channels such as ϕ N \rightarrow $\Sigma^* K$, as well as those involving $\Lambda(1405)K \rightarrow \Lambda\pi K, \Sigma\pi K$. Consequently, the effects arising from these coupled channels are not visible in lattice calculations. The ϕ N interaction in the $^2S_{1/2}$ state differs since it can couple via S-wave to the ΛK ($^2S_{1/2}$) and ΣK ($^2S_{1/2}$) states [18]. Such decay processes are described through kaon exchange, which introduces an imaginary component to the potential in the $^2S_{1/2}$ channel.

Conversely, the long-range TPE potential observed in the $^4S_{3/2}$ channel is expected to also characterize the $^2S_{1/2}$ channel. This is because the exchange of two pions in a scalar-isoscalar state does not depend on the total spin of the ϕ N system.

Based on the results presented in Refs. [18, 29], a fit was performed to experimental correlation data [30], constraining the spin 3/2 interaction using the scattering length obtained from lattice QCD simulations [18]. These considerations lead to the proposed potential form for the ϕ N system in the ${}^2S_{1/2}$ channel [30]:

$$V_{\phi N}(r) = \beta \left(\sum_{i=1}^2 a_i e^{-(r/b_i)^2} \right) + a_3 m_\pi^4 f(r; b_3) \left(\frac{e^{-m_\pi r}}{r} \right)^2 + i\gamma f(r; b_3) \frac{e^{-2m_K r}}{m_K r^2}, \quad (10)$$

where β and γ are parameters adjusted to fit experimental data; a_i and b_i are common to both the ${}^4S_{3/2}$ and ${}^2S_{1/2}$ channels, obtained through fits to lattice QCD data in the spin 3/2 channel at $t/a = 14$ [18] and $t/a = 12$ [30], respectively. These parameter values are listed in Table I. Here, t/a represents Euclidean (imaginary) time with a lattice spacing of $a = 0.0846$ fm.

In fact, in Ref. [30], the $t/a = 12$ value was chosen over the default $t/a = 14$ used in [18] to adopt a conservative approach, as it corresponds to the least attractive potential in the spin 3/2 channel, and consequently, to the weakest potential in the spin 1/2 channel. The function $f(r; b_3) = \left(1 - e^{-(r/b_3)^2}\right)^2$ is an Argonne-type form factor, discussed in [18].

For $\beta = 1$ and $\gamma = 0$, the potential in Eq. (10) reduces to the lattice QCD potential for the spin 3/2 channel [18]. Conversely, the fitted parameters $\beta = 6.9_{-0.5}^{+0.9}$ (stat.) $_{-0.1}^{+0.2}$ (syst.) and $\gamma = 0.0_{-3.6}^{+0.0}$ (stat.) $_{-1.8}^{+0.0}$ (syst.) are extracted through fitting to the experimental $p\phi$ correlation data measured by the ALICE collaboration in pp collisions at $\sqrt{s} = 13$ TeV [29].

In addition, in Ref. [30], physical masses were employed for both $m_\pi = 138$ MeV/ c^2 and $m_K = 496$ MeV/ c^2 to accurately model the experimental correlation function; similarly, the physical masses are used here. The HAL QCD ϕ N two-body potential in the ${}^4S_{3/2}$ channel (as given in Eq. (10) with parameters listed in Table I) does not produce a bound state. However, the ϕ N system in the ${}^2S_{1/2}$ channel is strongly bound, with a central binding energy of $B_{\phi N} = 28.93$ MeV at $t/a = 12$ [30], and 16.64 MeV at $t/a = 14$ [18].

TABLE I: The parameters of ϕ N potential given in Eq. (10) at lattice Euclidean time 12 [30] and 14 [18]. The numbers in parentheses indicate statistical errors.

| t/a | a_1 (MeV) | b_1 (fm) | a_2 (MeV) | b_2 (fm) | $a_3 m_\pi^4$ (MeV · fm ²) | b_3 (fm) |
|-------|-------------|------------|-------------|------------|--|------------|
| 12 | -392(10) | 0.128(3) | -145(9) | 0.284(7) | -83(1) | 0.582(6) |
| 14 | -371(27) | 0.13(1) | -119(39) | 0.30(5) | -97(14) | 0.63(4) |

In Fig. 2, the spin-averaged ϕ N potentials, as defined by Eq. (12), are displayed at time slices $t/a = 12$ and 14 using the parameters listed in Table I to facilitate better comparison.

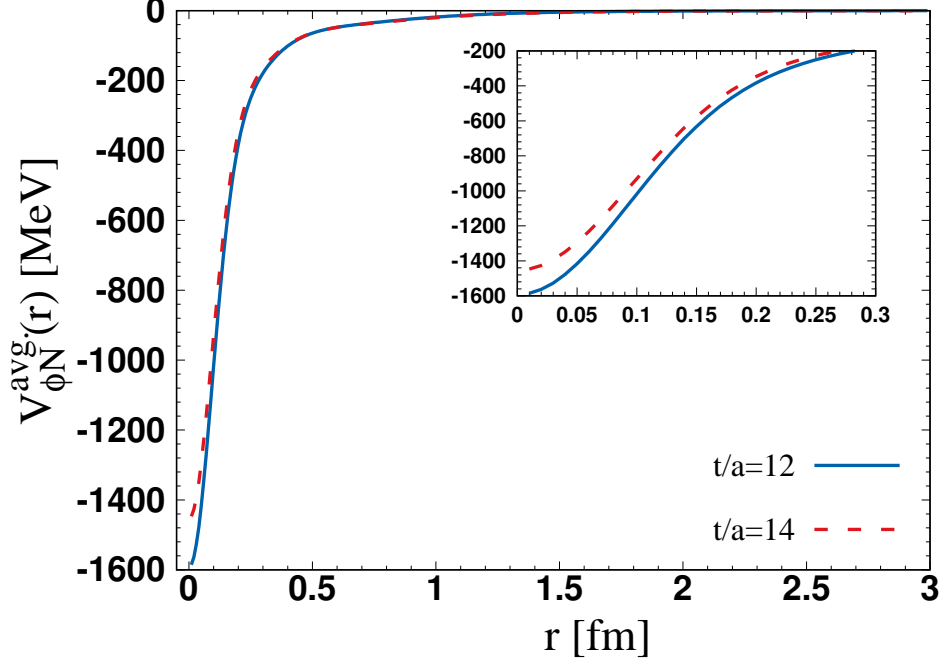


FIG. 2: The spin-averaged ϕ N potential in Eq. (12), as a function of separation r for lattice Euclidean times $t/a = 12$ (blue solid line), and 14 (red dashed lines) by the parameters given in Table I.

B. Construction of $\phi\alpha$ potential

The spin-averaged WS type form of the potential,

$$U_{\phi\alpha}^{fit}(r) = -U_0 \left[1 + \exp\left(\frac{r - R_{\phi\alpha}}{t_{\phi\alpha}}\right) \right]^{-1}, \quad (11)$$

for the $\phi\alpha$ potential, $U_{\phi\alpha}$, is obtained within the framework of the single-folding potential (SFP) approach. In this approach, the effective $\phi\alpha$ nuclear potential is estimated through the single folding of the nucleon density in the α -particle with the spin-averaged ϕ N interaction [7, 39–41]. The spin-averaged ϕ N potential is defined as

$$V_{\phi N}^{avg.}(r) = \frac{2}{3}V_{\phi N}(^4S_{3/2}) + \frac{1}{3}V_{\phi N}(^2S_{1/2}), \quad (12)$$

where the potential in the ${}^2S_{1/2}$ channel is notably more attractive in the short-range part due to the enhanced β , and the long-range tail is similar to that of the ${}^4S_{3/2}$ channel, arising from two-pion exchange [30]. It should be noted that, in Ref. [7], the $U_{\phi\alpha}$ potentials were constructed solely by folding the ϕ N potential in the ${}^4S_{3/2}$ channel. To achieve higher computational accuracy, such an approach is not adopted here.

Recently, the root-mean-square (rms) matter radius of ${}^4\text{He}$ was measured to be 1.70 ± 0.14 fm through analyses of near-threshold ϕ -meson photoproduction data from the LEPS Collaboration [42, 43]. These studies indicate that the rms charge radius of ${}^4\text{He}$ is smaller than the rms matter radius; however, the two quantities are statistically compatible within their error margins. Despite this apparent discrepancy, the densities used in our folding potential calculations are modeled to reproduce an rms radius of 1.70 fm.

TABLE II: The fit parameters for $U_{\phi\alpha}$ in Eq. (11) are obtained in conjunction with their corresponding central binding energy, $B_{\phi\alpha}$. The fitting range is selected for $r \gtrsim 1.70$ fm [44]. Calculations are performed using the experimental masses: $m_\alpha = 3727.38$ MeV/ c^2 and $m_\phi = 1019.5$ MeV/ c^2 . In Ref. [7], a $B_{\phi\alpha}$ value of 4.78 MeV is reported, with the $\phi\alpha$ potential constructed based solely on the $\phi\alpha$ interaction in the ${}^4S_{3/2}$ channel, and the rms radius set at 1.70 fm.

| t/a | U_0 (MeV) | $R_{\phi\alpha}$ (fm) | $t_{\phi\alpha}$ (fm) | $B_{\phi\alpha}$ (MeV) |
|-----|-------------|-----------------------|-----------------------|------------------------|
| 12 | 71.1 | 1.270 | 0.476 | 10.29 |
| 14 | 72.5 | 1.290 | 0.485 | 11.38 |

C. Choice of N-core interaction

Two types of $N\alpha$ interactions were tried. Both fit $N\alpha$ scattering phase shifts [45] satisfactorily. The first, SBB $V_{n\alpha}$ potential [34] has a Gaussian form given by

$$V_{n\alpha}(r) = \sum_{l=0,1,2} v^{(l)} \exp[-(r/b)^2] + v^{(ls)} \exp[-(r/b)^2], \quad (13)$$

having s -, p -, d - and ls components of different strengths but of a common range $b = 2.35$ fm. The strength parameters of the original SBB potential in MeV for different components are $v^{(s)} = 50.0$, $v^{(p)} = 47.32$, $v^{(d)} = -23.0$ and $v^{(ls)} = -11.71$ respectively. The repulsive

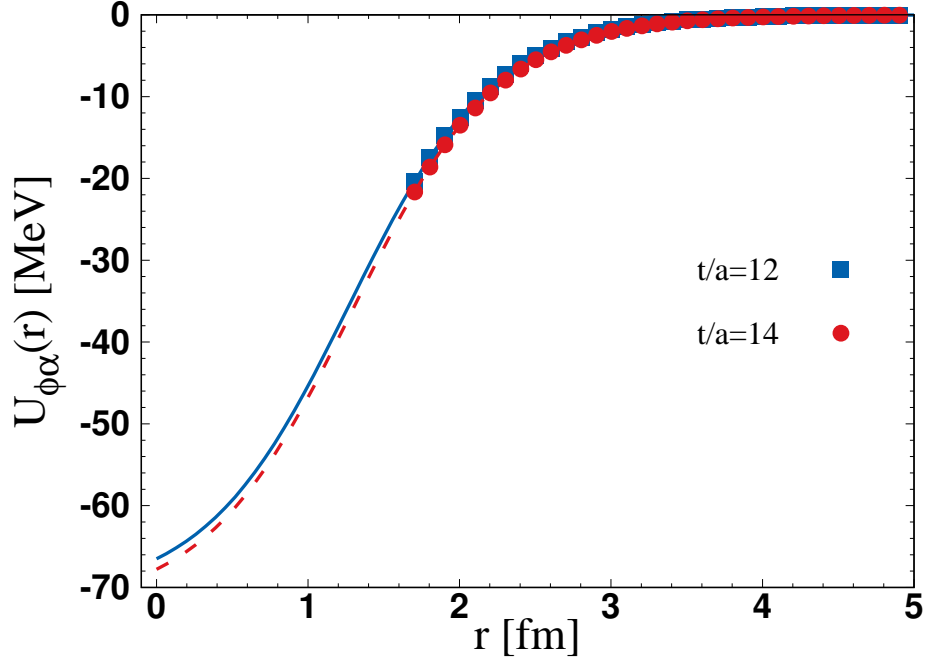


FIG. 3: The spin-averaged $\phi\alpha$ potential in Eq. (11) as a function of separation r for lattice Euclidean time $t/a = 12$ (blue solid line), and 14 (red dashed lines) by the parameters given in Table II.

s-component in the core(α)-N potential has been introduced to simulate Pauli principle between valence neutrons and nucleons forming the core nuclei.

The second choice $V_{n\alpha}$ (WS) employs a Woods-Saxon form for the corresponding potential components as used in the coordinate space Faddeev calculation [31, 35] for ${}^6\text{Li}$, and from Refs. [46, 47], with central $V_c(r)$ and spin-orbit $V_{so}(r)$ terms which are expressed as Woods-Saxon potentials,

$$V_c(r) = \frac{v_c^{(l)}}{1 + \exp\left(\frac{r-r_c^{(l)}}{a_c^{(l)}}\right)}, \quad (14)$$

$$V_{so}(r) = \frac{v_{so}}{ra_{so}} \frac{\exp\left(\frac{r-r_{so}}{a_{so}}\right)}{\left[1 + \exp\left(\frac{r-r_{so}}{a_{so}}\right)\right]^2}. \quad (15)$$

Again, the parameters for the central part are l -dependent, $v_c^{(s)} = 48.0$, $v_c^{(p)} = -43.0$, $v_c^{(d)} = -21.5$ MeV with same $r_c^{(s,p,d)} = 2.0$ fm and $a_c^{(s,p,d)} = 0.7$ fm. The spin-orbit potential parameters are given by: $v_{so} = -40.0$ MeV fm², $r_{so} = 1.5$ fm and $a_{so} = 0.35$ fm.

IV. NUMERICAL RESULTS

The numerical results for the ground state central binding energy, denoted as B_3 , and the nuclear matter radius, r_{mat} , for three-body $\phi\text{N-}\alpha$ systems are presented and discussed herein. The coupled equations, Eqs. (7) were solved using the FaCE computational toolkit [37], with the two-body interactions described in Sec. III.

In the HH method, the final results are dependent on the maximum hypermomentum value, K_{max} , due to the truncation of the total three-body wave function expansion in hypermomentum components. Therefore, an initial investigation into the convergence of results was performed as a function of K_{max} and the maximum number of hyperradial excitations, i_{max} . For the $\phi\text{N-}\alpha$ state, convergence was achieved satisfactorily with $K_{max} = 70$ and $i_{max} = 25$.

The HAL QCD ϕN two-body potential in the ${}^4S_{3/2}$ channel (Eq. (10) with parameters provided in Table I) was found not to form a bound state. In contrast, the ϕN interaction in the ${}^2S_{1/2}$ channel results in a strongly bound state, with central binding energies of 28.93 MeV and 16.64 MeV at lattice Euclidean times $t/a = 12$ [30] and 14 [18], respectively.

The ground state central binding energies and nuclear matter radii of $\phi\text{N-}\alpha$ mesic nuclei within the ${}^4S_{3/2}$ and ${}^2S_{1/2}$ spin channels are provided in Table III. The central binding energies of the $\phi\text{N-}\alpha$ bound states in the spin 3/2 (1/2) channel are found to be about 10 (25) and 11 (13) MeV at Euclidean times $t/a = 12$ and 14, respectively. A significant discrepancy has been observed between the binding energies of the $\phi\text{N-}\alpha$ (${}^2S_{1/2}$) state at Euclidean times $t/a = 12$ (25 MeV) and $t/a = 14$ (13 MeV). This difference is directly associated with the binding energies of the two-body ϕN systems at $t/a = 12$ and 14, which are approximately 29 MeV and 17 MeV, respectively, as noted in the preceding paragraph.

Furthermore, in order to compute the root-mean-square (rms) matter radius of the $\phi\text{N-}\alpha$ state, the rms matter radius of the α particle, taken as 1.7 fm [43], along with the strong interaction radius of the neutron (0.80 fm) and the ϕ -meson (0.46 fm) [17, 48], has been utilized in the calculation. The resulting nuclear matter radii of the $\phi\text{N-}\alpha$ bound states in the spin 3/2 (1/2) channels are estimated to be approximately 4.5 (1.7) fm and 4.6 (1.8) fm at Euclidean times $t/a = 12$ and $t/a = 14$, respectively.

TABLE III: Three-body ground state central binding energies (B_3) and the nuclear matter radii (r_{mat}) of the $\phi\text{N}-\alpha$ system for ϕN potentials in ${}^4S_{3/2}$ and ${}^2S_{1/2}$ channels, and two types of $\text{N}\alpha$ interactions, i.e., the SBB potential that is given by Eq. (13) and WS potential which is set by Eqs. (14), (15).

| $\text{N}\alpha$: | | SBB | | WS | |
|--------------------|---------------------|-------------|-----------------------|-------------|-----------------------|
| t/a | ϕN spin | B_3 (MeV) | r_{mat} (fm) | B_3 (MeV) | r_{mat} (fm) |
| 12 | ${}^4S_{3/2}$ | 9.68 | 4.55 | 8.70 | 3.45 |
| | ${}^2S_{1/2}$ | 25.21 | 1.71 | 25.10 | 1.70 |
| 14 | ${}^4S_{3/2}$ | 10.80 | 4.59 | 9.84 | 3.45 |
| | ${}^2S_{1/2}$ | 13.36 | 1.79 | 13.32 | 1.78 |

V. SUMMARY AND CONCLUSIONS

A new approach to studying the two-body ϕN interaction, particularly its spin dependence, has been investigated through the analysis of bound states in the $\phi\text{N}-\alpha$ mesic nuclei systems. In this approach, the α cluster is utilized to attract the ϕN pair without altering its spin configuration. The $\phi\alpha$ potential is constructed by applying a folding procedure to the spin-averaged ϕN interaction, combined with the matter distribution of ${}^4\text{He}$. Subsequently, the coupled Faddeev equations in coordinate space are solved within the hyperspherical harmonics expansion method, using the two-body potentials for each particle (cluster) pair.

The calculations employ the state-of-the-art ϕN potential derived from lattice QCD computations and correlation function analysis, specifically for the ${}^4S_{3/2}$ and ${}^2S_{1/2}$ channels. The $\text{N}\alpha$ interaction potential is modeled using two commonly adopted forms from the literature: one with a Gaussian profile (SBB) and the other with a Woods-Saxon profile, both including central and spin-orbit components.

The central binding energies of the $\phi\text{N}-\alpha$ bound states in the spin $3/2$ ($1/2$) channel are calculated to be about 10 (25) and 11 (13) MeV at Euclidean times $t/a = 12$ and 14, respectively. As well as, the corresponding nuclear matter radii are estimated to be about 4.5 (1.7) and 4.6 (1.8) fm.

Lattice calculations of the ϕN interaction in the ${}^4S_{3/2}$ channel are used in [30] to constrain the spin-1/2 (${}^2S_{1/2}$) channel by fitting the experimental ϕN correlation function measured

by the ALICE Collaboration [29]. For a meaningful comparison between theory and experiment, it is necessary to extract complex-valued scattering parameters in both the $^4S_{3/2}$ and $^2S_{1/2}$ channels through a coupled-channel analysis [22, 23] of the data from physical-point simulations [24]. It is hoped that the presented numerical results will aid in the planning of future experiments.

-
- [1] S. Hirenzaki and J. Yamagata-Sekihara, Formation of Slow Heavy Mesons in Nuclei, *Nucl. Phys. A* **835**, 406 (2010), proceedings of the 10th International Conference on Hypernuclear and Strange Particle Physics.
- [2] J. Yamagata-Sekihara, D. Cabrera, M. J. Vicente Vacas, and S. Hirenzaki, Formation of φ Mesic Nuclei, *Prog. Theor. Phys.* **124**, 147 (2010), <https://academic.oup.com/ptp/article-pdf/124/1/147/9681103/124-1-147.pdf>.
- [3] J. J. Cobos-Martínez, K. Tsushima, G. Krein, and A. W. Thomas, Φ -meson–nucleus bound states, *Phys. Rev. C* **96**, 035201 (2017).
- [4] H. Gao, H. Huang, T. Liu, J. Ping, F. Wang, and Z. Zhao, Search for a hidden strange baryon-meson bound state from ϕ production in a nuclear medium, *Phys. Rev. C* **95**, 055202 (2017).
- [5] F. Etminan and A. Aalimi, Examination of the ϕ – NN bound-state problem with lattice QCD N – ϕ potentials, *Phys. Rev. C* **109**, 054002 (2024).
- [6] I. Filikhin, R. Y. Kezerashvili, and B. Vlahovic, Possible $^3_\phi\text{H}$ hypernucleus with the HAL QCD interaction, *Phys. Rev. D* **110**, L031502 (2024).
- [7] I. Filikhin, R. Y. Kezerashvili, and B. Vlahovic, Bound states of $^9_\phi\text{Be}$ and $^6_\phi\text{He}$ within $\phi + \alpha + \alpha$ and $\phi + \phi + \alpha$ cluster models, *Phys. Rev. C* **110**, 065202 (2024).
- [8] F. Etminan, Exploring the ϕ – α interaction via femtosopic study, *Phys. Lett. B* **866**, 139564 (2025).
- [9] P. Gubler, Studies on the ϕ meson production in nuclear matter and the ϕN correlation function, *Journal of Subatomic Particles and Cosmology* **1-2**, 100007 (2024).
- [10] P. Achenbach *et al.*, Mini-Proceedings of the "Fourth International Workshop on the Extension Project for the J-PARC Hadron Experimental Facility (HEF-ex 2024)", (2024), [arXiv:2409.00366](https://arxiv.org/abs/2409.00366) [nucl-ex].

- [11] D. Cabrera, A. N. Hiller Blin, and M. J. Vicente Vacas, ϕ meson self-energy in nuclear matter from ϕN resonant interactions, *Phys. Rev. C* **95**, 015201 (2017).
- [12] J. Kim, P. Gubler, and S. H. Lee, ϕ meson properties in nuclear matter from QCD sum rules with chirally separated four-quark condensates, *Phys. Rev. D* **105**, 114053 (2022).
- [13] L. M. Abreu, P. Gubler, K. Khemchandani, A. Martínez Torres, and A. Hosaka, A study of the ϕN correlation function, *Phys. Lett. B* **860**, 139175 (2025).
- [14] V. B. Belyaev, W. Sandhas, and I. I. Shlyk, New nuclear three-body clusters ϕNN , *Few-Body Syst.* **44**, 347 (2008).
- [15] V. B. Belyaev, W. Sandhas, and I. I. Shlyk, 3- and 4- body meson- nuclear clusters (2009), [arXiv:0903.1703v1 \[nucl-th\]](https://arxiv.org/abs/0903.1703v1).
- [16] S. A. Sofianos, G. J. Rampho, M. Braun, and R. M. Adam, The $\phi - NN$ and $\phi\phi - NN$ mesic nuclear systems, *J. Phys. G Nucl. Part. Phys.* **37**, 085109 (2010).
- [17] X.-Y. Wang, C. Dong, and Q. Wang, First characterization of the scattering length distribution of the vector meson interaction with the deuteron, *Phys. Rev. C* **108**, 034614 (2023).
- [18] Y. Lyu, T. Doi, T. Hatsuda, Y. Ikeda, J. Meng, K. Sasaki, and T. Sugiura, Attractive $N-\phi$ interaction and two-pion tail from lattice QCD near physical point, *Phys. Rev. D* **106**, 074507 (2022).
- [19] J. J. Krauth *et al.*, Measuring the α -particle charge radius with muonic helium-4 ions, *Nat.* **589**, 527 (2021).
- [20] N. Ishii *et al.* (HAL QCD Collaboration), Hadron-hadron interactions from imaginary-time Nambu-Bethe-Salpeter wave function on the lattice, *Phys. Lett. B* **712**, 437 (2012).
- [21] S. Aoki, B. Charron, T. Doi, T. Hatsuda, T. Inoue, and N. Ishii, Construction of energy-independent potentials above inelastic thresholds in quantum field theories, *Phys. Rev. D* **87**, 034512 (2013).
- [22] S. Kenji *et al.* (HAL QCD Collaboration), $\Lambda\Lambda$ and $N\Xi$ interactions from lattice QCD near the physical point, *Nucl. Phys. A* **998**, 121737 (2020).
- [23] F. Etminan, K. Sasaki, and T. Inoue, Coupled-channel $\Lambda_c K^+ - p D_s$ interaction in the flavor SU(3) limit of lattice QCD, *Phys. Rev. D* **109**, 074506 (2024).
- [24] T. Aoyama, T. M. Doi, T. Doi, E. Itou, Y. Lyu, K. Murakami, and T. Sugiura (HAL QCD collaboration), Scale setting and hadronic properties in the light quark sector with (2+1)-flavor Wilson fermions at the physical point, *Phys. Rev. D* **110**, 094502 (2024).

- [25] T. Iritani *et al.*, $N\Omega$ dibaryon from lattice QCD near the physical point, *Phys. Lett. B* **792**, 284 (2019).
- [26] S. Gongyo *et al.* (HAL QCD Collaboration), Most strange dibaryon from lattice QCD, *Phys. Rev. Lett.* **120**, 212001 (2018).
- [27] Y. Lyu, H. Tong, T. Sugiura, S. Aoki, T. Doi, T. Hatsuda, J. Meng, and T. Miyamoto, Dibaryon with Highest Charm Number near Unitarity from Lattice QCD, *Phys. Rev. Lett.* **127**, 072003 (2021).
- [28] Y. Lyu, T. Doi, T. Hatsuda, and T. Sugiura, Nucleon-charmonium interactions from lattice QCD, *Phys. Lett. B* **860**, 139178 (2025).
- [29] S. Acharya *et al.* (ALICE Collaboration), Experimental Evidence for an Attractive $p-\phi$ Interaction, *Phys. Rev. Lett.* **127**, 172301 (2021).
- [30] E. Chizzali, Y. Kamiya, R. Del Grande, T. Doi, L. Fabbietti, T. Hatsuda, and Y. Lyu, Indication of a $p-\phi$ bound state from a correlation function analysis, *Phys. Lett. B* **848**, 138358 (2024).
- [31] M. Zhukov *et al.*, Bound state properties of Borromean halo nuclei: ${}^6\text{He}$ and ${}^{11}\text{Li}$, *Phys. Rep.* **231**, 151 (1993).
- [32] J. Casal, J. Singh, L. Fortunato, W. Horiuchi, and A. Vitturi, Electric dipole response of low-lying excitations in the two-neutron halo nucleus ${}^{29}\text{F}$, *Phys. Rev. C* **102**, 064627 (2020).
- [33] F. Etminan, Z. Sanchuli, and M. M. Firoozabadi, Geometrical properties of ΩNN three-body states by realistic NN and first principles Lattice QCD ΩN potentials, *Nucl. Phys. A* **1033**, 122639 (2023).
- [34] S. Sack, L. C. Biedenharn, and G. Breit, The Elastic Scattering of Protons by Alpha Particles, *Phys. Rev.* **93**, 321 (1954).
- [35] J. Bang, J.-J. Benayoun, C. Gignoux, and I. Thompson, Scattering and break-up of deuterons on α -particles in a realistic three-body model, *Nucl. Phys. A* **405**, 126 (1983).
- [36] J. Raynal and J. Revai, Transformation coefficients in the hyperspherical approach to the three-body problem, *Il Nuovo Cimento A (1965-1970)* **68**, 612 (1970).
- [37] I. Thompson, F. Nunes, and B. Danilin, FaCE: a tool for three body Faddeev calculations with core excitation, *Comput. Phys. Commun* **161**, 87 (2004).
- [38] J. A. Lay, A. M. Moro, J. M. Arias, and J. Gómez-Camacho, Particle motion in a deformed potential using a transformed oscillator basis, *Phys. Rev. C* **85**, 054618 (2012).

- [39] G. Satchler and W. Love, Folding model potentials from realistic interactions for heavy-ion scattering, [Phys. Rep. **55**, 183 \(1979\)](#).
- [40] K. S. Myint and Y. Akaishi, Double-Strangeness Five-Body System, [Prog. Theor. Phys. **117**, 251 \(1994\)](#).
- [41] F. Etminan and M. M. Firoozabadi, Simple Woods-Saxon type form for $\Omega\alpha$ and $\Xi\alpha$ interactions using folding model, [Chin. Phys. C **44**, 054106 \(2020\)](#).
- [42] T. Hiraiwa *et al.* (LEPS Collaboration), First measurement of coherent ϕ -meson photoproduction from ^4He near threshold, [Phys. Rev. C **97**, 035208 \(2018\)](#).
- [43] R. Wang, C. Han, and X. Chen, Exploring the mass radius of ^4He and implications for nuclear structure, [Phys. Rev. C **109**, L012201 \(2024\)](#).
- [44] I. Filikhin, R. Y. Kezerashvili, and B. Vlahovic, Folding Procedure for Ω - α Potential, [Few-Body Syst. **66**, 2 \(2024\)](#).
- [45] S. Ali, A. A. Z. Ahmad, and N. Ferdous, A survey of the alpha-nucleon interaction, [Rev. Mod. Phys. **57**, 923 \(1985\)](#).
- [46] I. J. Thompson, B. V. Danilin, V. D. Efros, J. S. Vaagen, J. M. Bang, and M. V. Zhukov, Pauli blocking in three-body models of halo nuclei, [Phys. Rev. C **61**, 024318 \(2000\)](#).
- [47] J. Casal, M. Rodríguez-Gallardo, and J. M. Arias, Analytical transformed harmonic oscillator basis for three-body nuclei of astrophysical interest: Application to ^6He , [Phys. Rev. C **88**, 014327 \(2013\)](#).
- [48] B. Povh and J. Hüfner, Systematics of strong interaction radii for hadrons, [Phys. Lett. B **245**, 653 \(1990\)](#).